6 (3): 251-259 (2022)

Journal of Aviation

https://dergipark.org.tr/en/pub/jav

e-ISSN 2587-1676

Effects of Shape Changing of Morphing Rotary Wing Aircraft on Longitudinal and Lateral Flight

Enes Özen[1*], Tuğrul Oktay[2]

[1*]Hasan Kalyoncu University, Vocational School, 27010, Gaziantep Türkiye. (enes.ozen@hku.edu.tr).
[2] Erciyes University, Faculty of Aeronautics and Astronautics, Kayseri, Türkiye. (oktay@erciyes.edu.tr).

Article Info

Received: February, 28. 2022
Revised: July, 04. 2022
Accepted: August, 02. 2022

Keywords:
Rotary Wing Aircraft
Morphing
State Space Model
PID

Corresponding Author: *Enes Özen*

RESEARCH ARTICLE

https://doi.org/10.30518/jav.1080139

Abstract

Unmanned aerial vehicles are aerial robots controlled by commands sent from the ground control station. While fixed-wing aircraft have the advantages of long range and high altitude, they need a runway to create sufficient lift on the wings. The advantage of Rotary Wing Aircraft is that it does not need a runway, it can perform vertical take-off and landing. It can hover. Thanks to these features, it is used in tasks such as surveillance, search and rescue, and reconnaissance. In areas with chemical wastes or in closed environments without risking the human element; Desired tasks can be performed in places such as sewers, caves, and collapsed houses. For this, there is a flight control computer and software on the aircraft. Rotary-wing aircraft are more unstable than fixed-wing aircraft. Thanks to the flight controller, its stability and controllability are increased. In this study, a quadcopter, multicopter aircraft structure is used. The variation of the angle between the arms of a quadcopter aircraft and its effects on forward and sideways flight are examined. It is required that the aircraft be symmetrical in the longitudinal and lateral axis in order to cope with the disturbances to which it is exposed in external environments. In closed environments, atmospheric events are replaced by obstacles. One of the desirable features of the aircraft is that it can pass through narrow places. For this, the aircraft must perform a shape change. The change in structure will cause it to change in the dynamic's equations, causing the rotors to react differently during linear and rotational movements of the aircraft. This study focuses on the system design and control of the aircraft. The geometric features obtained from the aircraft designed in the CATIA program were used in the creation of the mathematical model. The obtained values were created using the MATLAB Simulink program to create a digital twin of the aircraft. When the intersection angle between the arms is 90 degrees, the settling time of the 2-degree pitch angle is 7.48 seconds, and when it is 45 degrees, it is 10.3 seconds.

1. Introduction

Unmanned aerial vehicles (UAVs) are aircraft that are autonomous or controlled by commands transmitted from a ground control station. It consists of classes such as fixed-wing and rotary-wing aircraft. Rotary-wing aircraft are classified by the word ' copter ', which derives from the ancient Greek word ' pteron '. This classification is named according to the number of propellers it has (Boulet, 1991). These are tricopter, quadcopter, hexacopter, octocopter and helicopter. Rotary wing aircraft are of unstable structure and flight control card and flight control software are used in order to be stable and controllable. Its job is to control the rotors and actuators and to make the movement happen. There is no cockpit and pilot on the unmanned aerial vehicle. Control is provided by modulating the commands sent from the ground control station to radio waves and capturing the waves of the antenna on the aircraft. The information is transmitted from the antenna to the receiver and demodulated to the relevant avionics' element. The information sent from the ground is processed by the flight control card (FCC) and transmitted (TX) to the rotors, the rotation speed of the rotors is controlled (Coban et al., 2019). As with manned aircraft, unmanned aerial vehicles have control surfaces and propulsion system to perform linear and rotational movements. However, control is transmitted by the operator in the ground control station, not by the pilot in the cockpit. Unmanned aerial vehicles have become a popular topic (Coban et al., 2020) thanks to the development and accessibility of electronics, software and material technology. It is widely used in civil and military aviation. Generally, these systems are used for outdoor scenarios. Indoor applications; cave, rescue in collapsed buildings, intervening in terrorist activities in closed areas are some of them (Desbiez et al., 2017). This often involves traveling between small cracks or gaps in confined spaces; they cause situations that are very difficult for conventional quadcopter aircraft, possibly resulting in catastrophe (Falanga et al., 2018). It enables it to pass through narrow spaces by imitating the birds that can be observed in nature (Di Luca et al., 2017). Thanks to image identification, sensor fusion and artificial intelligence applications, it can be made suitable for indoor use (Bai et al., 2019). These are according to the obstacles; It is to change the shape of the quadcopter aircraft, to prevent collisions and to provide a more suitable shape. In quadcopter unmanned aerial vehicles, shaping is done by methods such as arm extension or shortening, or by changing the angles between

the arms (Köse et al. 2020; Oktay et al., 2021) It can be used as a morphing control element to change flight dynamics (Prisacariu, et al., 2011). If morphing is done before the flight of the Four Propellers, it is called passive morphing. If morphing occurs during flight, this type is called active morphing (Oktay et al., 2016). In this study, studies that perform active and passive morphing (Oktay et al., 2017) were examined and modeling and simulation were carried out.

There is a mechanism structure that can rotate around the z axis at the intersection point of the two arms of the vehicle and the arms (Figure 1). The intersection angle is driven by the actuator (Figure 3), allowing the vehicle to expand and contract. In this case, changes in vehicle dynamics are controlled by the designed controller.

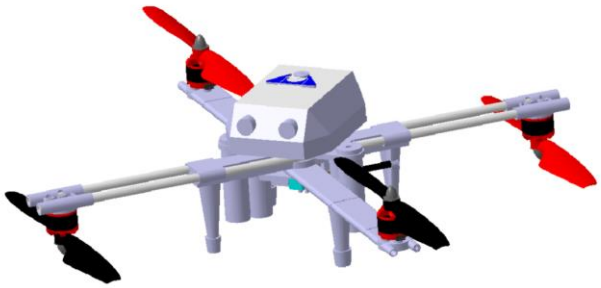

Figure 1. X1 Non-Morphing Configuration

2. Materials and Methods

The position, velocity and acceleration information of the moving objects are calculated by means of the sensors on it. These are elements such as GPS, accelerometer, gyroscope, telemetry, 3D flow camera, INS. In the INS system, it does not need to communicate or reference any station on the ground or in space. It is the only long-range navigation system that does not use radio waves. It works in conjunction with a computer and works completely independently. The ability of the aircraft to travel from one point to another by the shortest route serves the purpose of determining its position and location at any time of the flight (Kekeç et al. 2020).

According to the kinematic theory, all the motion parameters of an object in motion can be easily calculated if its acceleration, initial position and velocity at every instant are known. Two sets of axes are used for this. These are the fixed pivot assembly and the body pivot assembly. The aircraft is calibrated at the starting point and matched with the fixed axis set. After that, each movement is calculated by the accelerometer and gyroscope on the aircraft and position information is obtained (Köse et al., 2021).

2.1. Quadcopter Features

The rotary-wing unmanned aerial vehicle takes off with the lift force obtained by the rotors turning the propellers (Eraslan et al., 2020). The rotation of the rotor at different speeds, the rotation movements performed in the fuselage axis set in the center of the aircraft, enable it to move in the horizontal or vertical axis. This change in the angular velocity of the rotors transmits a signal to the rotors to provide the necessary orientation by the flight controller from the sensors and the compilation of the commands (Oktay et al., 2021). The configuration information that determines the rotor placement and rotation directions of the quadcopter unmanned aerial vehicle is important. There are two types of configurations, plus and cross configurations. In this study, the X (cross) (Figure 2) configuration was preferred.

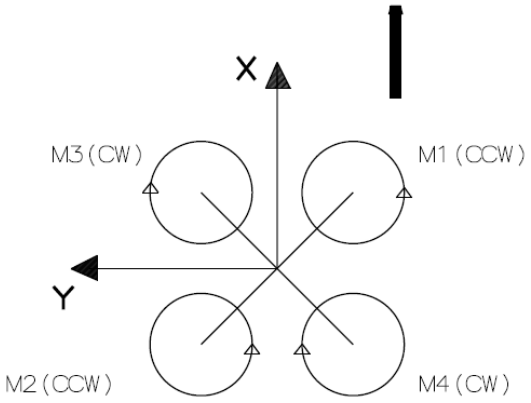

Figure 2. X Frame Configuration

The configuration information that determines the rotor placement and rotation directions of the quadcopter unmanned aerial vehicle is important. There are two types of configurations, plus and cross configurations. In this study, the X (cross) (Figure 2) configuration was preferred.

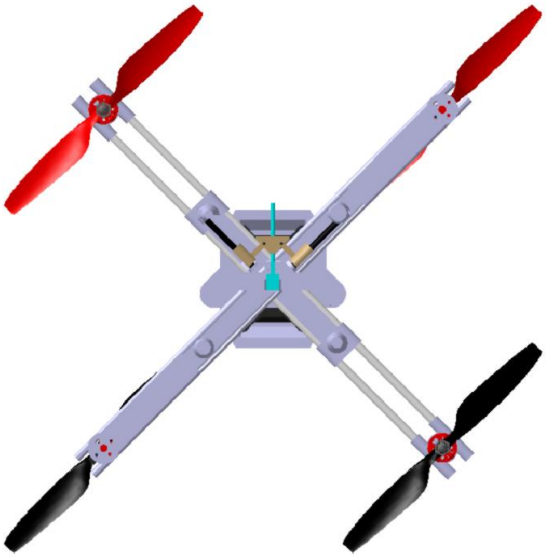

Figure 3. Quadcopter Bottom View

As seen in Figure 4, the aircraft moves the linear bearings on both arms with a fixed linear motor under the fuselage. As a result of the forward movement of the linear bearing, the angle between the arms decreases. The smallest value that the intersection angle can take is 45°. If the intersection angle is 45°, the configuration of the aircraft changes to X2. This situation changes the moment of inertia of the aircraft relative to the x-axis and y-axis. It changes the x and y distances of the rotation centers of the rotors from the center of gravity of the aircraft. It requires the change of dynamic forces on the aircraft and the updating of the mathematical model.

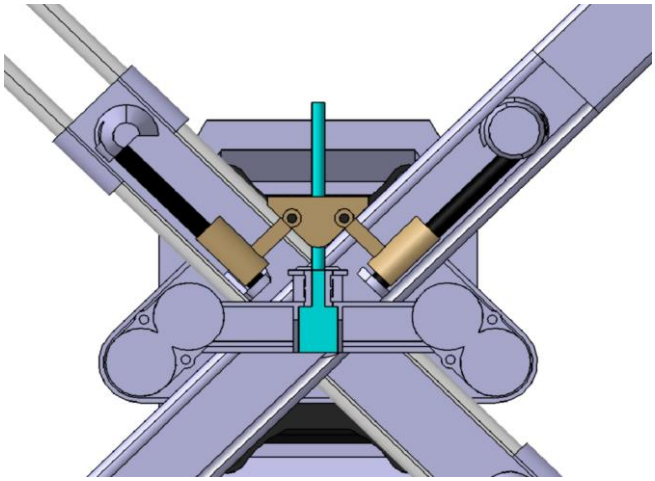

Figure 4. Quadcopter Bottom View-Mechanism

Batteries were placed vertically on both sides of the fuselage to act as a constraint during the variation of the intersection angle between the arms of the fuselage design of the aircraft. Li-ion 18650 battery cells have a voltage of 3.7 V. Sufficient voltage to create the necessary lifting force for the aircraft to fly was determined as 14.8 V. As seen in Figure 5, the required voltage was obtained by connecting the battery cells in series.

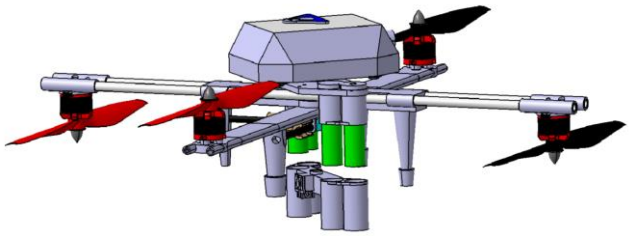

Figure 5. Quadcopter Battery Box Design – Li ion Battery

2.1. Quadcopter Moment of Inertia

In linear algebra, the diagonal matrix (↘) is a matrix whose entries outside the first diagonal are all zero and usually a square matrix. The matrix D = (di,j) consisting of n columns and n rows is as follows: If i≠j ∀i,j∈{1,2,….,n} then d_(i,j)=0. The structure of the aircraft is symmetrical. The mass distribution is considered homogeneous. The body axis is coincident with the center of gravity (1).

$$I = \text{diag}([\ Ixx\ Iyy\ Izz\ ]) \quad (1)$$

When the intersection angle of the aircraft changes, some values also change. This change affects the control of the rotation movements of the aircraft and the rotor rotation speeds. The general characteristics of the quadcopter aircraft are given in Table 1.

Table 1. X1 and X2 Configuration Geometries

Symbol	Definition	X1 Config	X2 Config	Unit
∠	Intersection Angle	90	45	degree
m	Aircraft Mass	750	750	gram
l	Arm Length	0.225	0.225	m

The angle of intersection between the arms of the quadcopter aircraft is 90 °. The link has 1 DOF movement around the z -axis. The angle between the arms can be changed by servo or linear actuator.

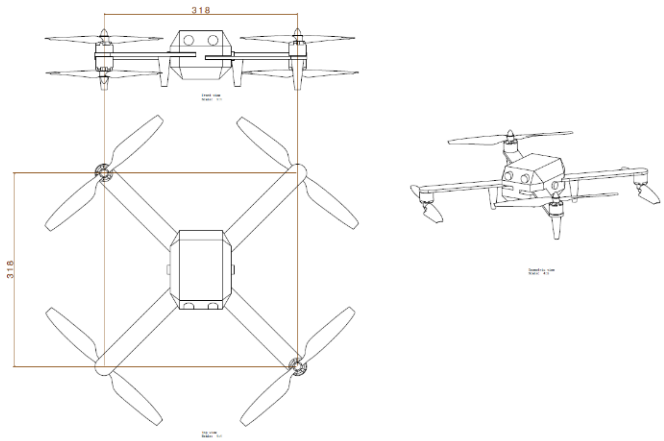

Figure 6.a) X1 Configuration Intersection Angle 90° (Non-Morphing)

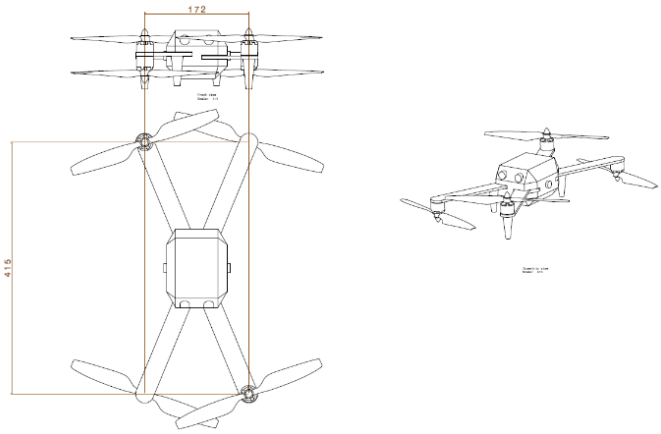

Figure 6.b) X2 Configuration Intersection Angle 45° (Morphing)

This change and its effect on moments of inertia are given in Table 2. Some assumptions were made while preparing the table. The structure of the aircraft is the joining of 2 arms with each other at their midpoints and the rotors mounted on the ends of each arm. Arm, fasteners, rotor and propellers; considered as homogeneous arm. The weight of each arm was calculated as m=0.75/4 kg. The moment of inertia of a homogeneous rod is calculated by equation (2).

$$I = \frac{1}{3}ml^2 \quad (2)$$

m; arm mass, l; arm length is accepted. Since the system is symmetrical, it is calculated from equation (1). l is accepted as the distance of the arms from the center in the x and y directions, and the system is considered symmetrical when the intersection angle is 90° (Figure 7). I_z when the intersection angle is 45° (Figure 8) does not change; I_x (decreasing), I_y (increasing) varies. Shape change function;

$$y = f(x) \quad (3)$$

In the function y; while the variable x defines the moments of inertia, it defines the intersection angle.

$$I_{x,y} = \frac{1}{3}ml^2 \sin\theta \quad (4)$$

Table 2, the change in the moment of inertia is obtained from equation (4).

Table 2. The Effect of Change in Intersection Angle of Laterally Contrasting Aircraft on Moment of Inertia

Symbol	Non-Morphing	Morphing	Unit
∠ /2	90	45	degree
m	0.75	0.75	kg
l	0.225	0.225	meter
w	0.318	0.172	meter
b	0.318	0.415	meter
I_x	0.005	0.003	kgm^2
I_y	0.005	0.008	kgm^2
I_z	0.009	0.009	kgm^2

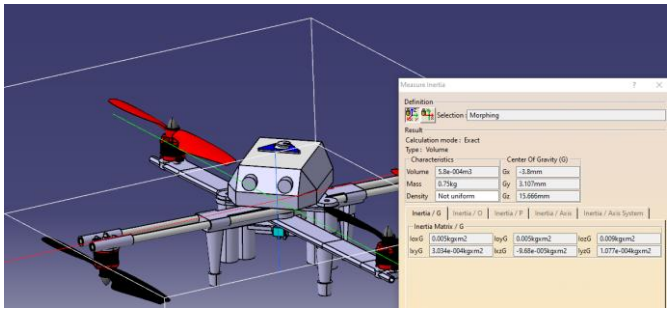

Figure 7. X1 Configuration Intersection Angle 90° (Non Morphing)

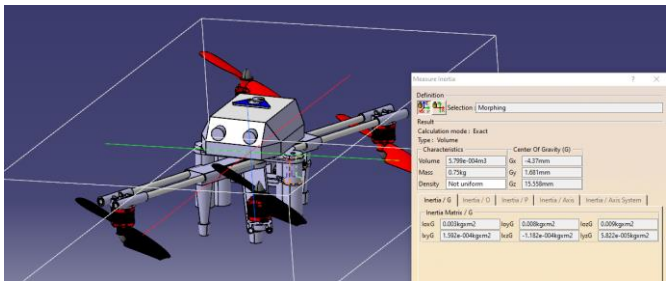

Figure 8. X2 Configuration Intersection Angle 45° (Morphing)

2.1. State Space Model

The obtained mathematical equations show that the quadcopter UAV is a multi-input multiple-output (MIMO) nonlinear system. In order to examine such a system, the state variables of the system must be determined. State space notation is used to express it with first-order differential equations (Köse et al., 2021)

$$\dot{x}=Ax(t)+Bu(t)$$
$$y=Cx(t)+Du(t) \quad (5)$$

Here, x(t) is the state vector (15), u(t) is the control or input vector (16), y(t) is the output vector, A is the system matrix, B is the input matrix, C is the output matrix, and D is the feedforward matrix. The state vector and control vector of the quadcopter are as given below.

$$x = [x\ \dot{x}\ y\ \dot{y}\ z\ \dot{z}\ \emptyset\ \dot{\emptyset}\ \theta\ \dot{\theta}\ \varphi\ \dot{\varphi}] \quad (6)$$

$$u = [U_1 U_2\ U_3\ U_4]^T \quad (7)$$

(8)

$$\begin{bmatrix} U_1 \\ U_2 \\ U_3 \\ U_4 \end{bmatrix} = \begin{bmatrix} b & b & b & b \\ \frac{-lb}{\sqrt{2}} & \frac{lb}{\sqrt{2}} & \frac{lb}{\sqrt{2}} & \frac{-lb}{\sqrt{2}} \\ \frac{lb}{\sqrt{2}} & \frac{-lb}{\sqrt{2}} & \frac{lb}{\sqrt{2}} & \frac{-lb}{\sqrt{2}} \\ d & d & -d & -d \end{bmatrix} \begin{bmatrix} \omega_1^2 \\ \omega_2^2 \\ \omega_3^2 \\ \omega_4^2 \end{bmatrix}$$

In this case, the quadcopter forward flight state space model would be as shown below. In the longitudinal state space model output matrix, the outputs followed in this study are given as outputs since z and θ are followed.

$$\begin{bmatrix} \dot{x} \\ \dot{z} \\ \dot{u} \\ \dot{w} \\ \dot{q} \\ \dot{\theta} \end{bmatrix} = \begin{bmatrix} 0 & 0 & 1 & 0 & 0 & 0 \\ 0 & 0 & 0 & 1 & 0 & 0 \\ 0 & 0 & 0 & 0 & 0 & -g \\ 0 & 0 & 0 & 0 & 0 & 0 \\ 0 & 0 & 0 & 0 & 0 & 0 \\ 0 & 0 & 0 & 0 & 1 & 0 \end{bmatrix} \begin{bmatrix} x \\ z \\ u \\ w \\ q \\ \theta \end{bmatrix} + \begin{bmatrix} 0 & 0 \\ 0 & 0 \\ 0 & 0 \\ 1/m & 0 \\ 0 & 1/I_y \\ 0 & 0 \end{bmatrix} \begin{bmatrix} U_1 \\ U_3 \end{bmatrix} \quad (9)$$

$$y = \begin{bmatrix} 0 & 0 & 0 & 0 & 0 & 0 \\ 0 & 1 & 0 & 0 & 0 & 0 \\ 0 & 0 & 0 & 0 & 0 & 0 \\ 0 & 0 & 0 & 0 & 0 & 0 \\ 0 & 0 & 0 & 0 & 0 & 0 \\ 0 & 0 & 0 & 0 & 0 & 1 \end{bmatrix} \begin{bmatrix} x \\ z \\ u \\ w \\ q \\ \theta \end{bmatrix}$$

The state space model represents the moment of inertia I_y in the input matrix. The moment of inertia is a diagonal matrix. This matrix is produced because the four arms of the Quadcopter are symmetrical and aligned on the x and y axes. The initial matrix is as shown in (1).

The lateral flight state space model is given as output because z and θ are followed in the output matrix.

$$\begin{bmatrix} \dot{y} \\ \dot{v} \\ \dot{p} \\ \dot{r} \\ \dot{\emptyset} \\ \dot{\varphi} \end{bmatrix} = \begin{bmatrix} 0 & 1 & 0 & 0 & 0 & 0 \\ 0 & 0 & 0 & 0 & g & 0 \\ 0 & 0 & 0 & 0 & 0 & 0 \\ 0 & 0 & 0 & 0 & 0 & 0 \\ 0 & 0 & 1 & 0 & 0 & 0 \\ 0 & 0 & 0 & 1 & 0 & 0 \end{bmatrix} \begin{bmatrix} y \\ v \\ p \\ r \\ \emptyset \\ \varphi \end{bmatrix} + \begin{bmatrix} 0 & 0 \\ 0 & 0 \\ 1/I_x & 0 \\ 0 & 1/I_z \\ 0 & 0 \\ 0 & 0 \end{bmatrix} \begin{bmatrix} U_2 \\ U_4 \end{bmatrix} \quad (10)$$

$$y = \begin{bmatrix} 0 & 0 & 0 & 0 & 0 & 0 \\ 0 & 0 & 0 & 0 & 0 & 0 \\ 0 & 0 & 0 & 0 & 0 & 0 \\ 0 & 0 & 0 & 0 & 0 & 0 \\ 0 & 0 & 0 & 0 & 1 & 0 \\ 0 & 0 & 0 & 0 & 0 & 0 \end{bmatrix} \begin{bmatrix} y \\ v \\ p \\ r \\ \emptyset \\ \varphi \end{bmatrix}$$

The state space model is I_x in the input matrix and I_z represents the moment of inertia . The moment of inertia is a diagonal matrix. This matrix is produced because the four arms of the Quadcopter are symmetrical and aligned on the x and y axes. The initial matrix is as shown in (1).

2.5. PID Control

Longitudinal movement, which is the movement in the y-axis for forward movement, is provided by control inputs U_3 . The four rotors perform their longitudinal movement between the values of π /2 and π /2. The PID equation for the quadcopter longitudinal motion can be written as:

$$U_3 = K_p e(t) + K_i \int_0^t e(t)dt + K_d \frac{de(t)}{dt} \quad (11)$$

For lateral movement, lateral movement, which is the movement in the x-axis, is provided by the U_2 and U_4 control inputs. It performs the four-rotor lateral movement between $-\pi$ and π values. The PID equation for quadcopter lateral motion can be written as:

$$U_2 = K_p e(t) + K_i \int_0^t e(t)dt + K_d \frac{de(t)}{dt} \quad (12)$$

3. Result and Discussion

Since this study is about forward flight and lateral flight, different flight characteristics are created by decreasing or increasing the intersection angle between the arms at different times. As the volume of the quadcopter changes during the conversion process, there are also changes in the moments of inertia. Usually, to reach the x and y positions, the roll and pitch angles are determined, which causes the quadcopter to steer the aircraft to that position, rather than sending a controller signal directly to its rotors. Assume that the body frame and the inertial frame coincide. In this case, when the roll angle is met, the quadcopter moves eastward ( ) on the globe; when it achieves a pitch attitude, it moves to the north ( ) direction on the earth. Thus, the controller designed to take the aircraft to the desired x and y positions is used to derive the roll and pitch angle requirements that must be made according to the current position. In order for the quadcopter to perform its longitudinal motion, U_3 given in equation (8) is applied as input. In the state space model, θ is shown as the output for the longitudinal motion. The Simulink model, designed for a 2° longitudinal angle, was examined under the headings of non-morphing and morphing. U_2 given in equation (8) is applied as input for the quadcopter to perform its lateral movement. In the state space model, $\emptyset$ it is shown as the output for its lateral movement. The Simulink model, designed for a lateral angle of 2°, was examined under the headings of non-morphing and morphing.

3.1. Non-Morphing

Simulated in MATLAB / Simulink using the values given in the Table 3 without changing the intersection angle between the arms of the aircraft. Matlab The block diagram in SIMULINK is as shown in the figure. Input data were obtained from u,w,q , pitch , X,Y graphs by entering the state space model.

Table 3. Overall Dimensions of the Aircraft (Intersection Angle; 90°)

Symbol	Non-Morphing	Unit
∠ /2	90	degree
m	0.75	kg
l	0.225	meter
w	0.318	meter
b	0.318	meter
I_x	0.005	kgm^2
I_y	0.005	kgm^2
I_z	0.009	kgm^2

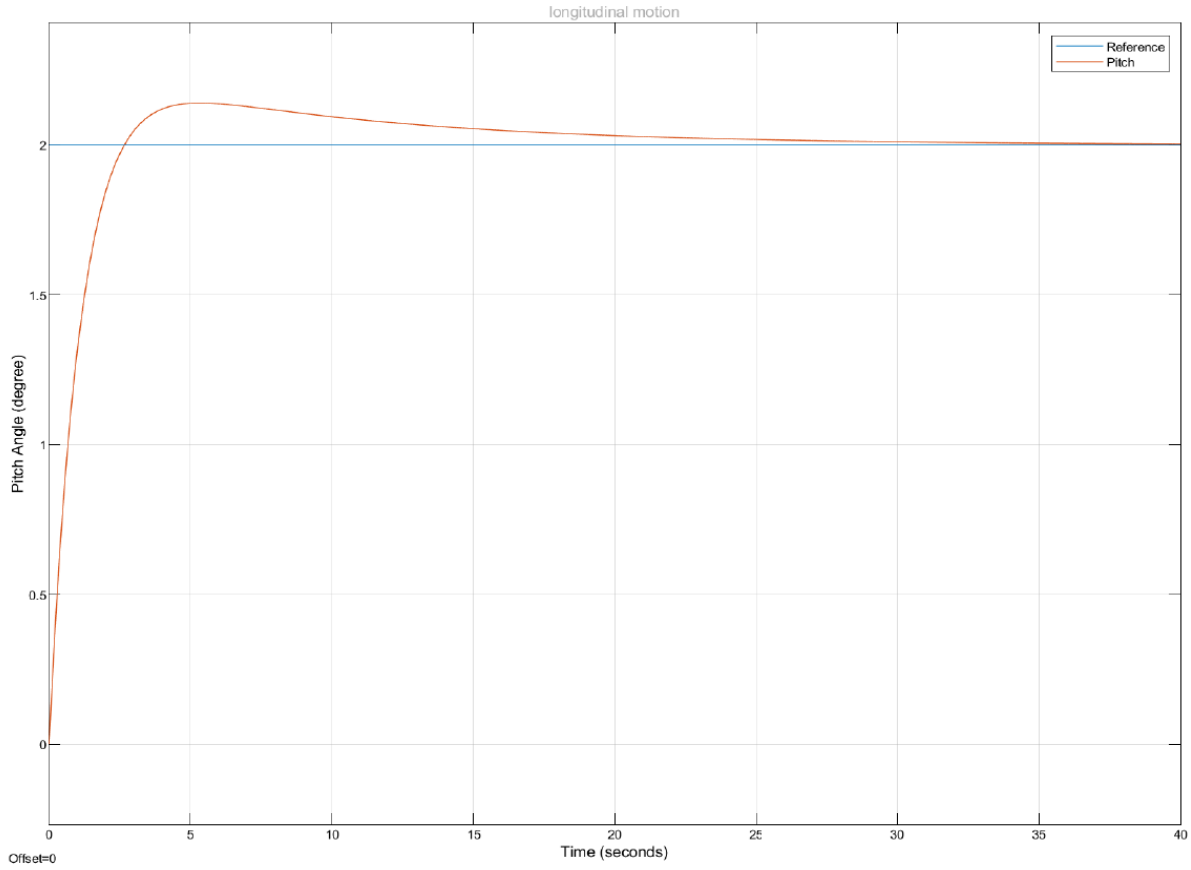

Figure 9. Forward Movement (Intersection Angle; 90°). PID (50,5,50)

In the simulation, an angle of 2° is given as a reference value. Longitudinal movement PID values P=50; I=5; Values were entered as D=50 by making use of previous studies (Oktay et al.,2017). The graph was obtained by running the simulation for 40 seconds. The longitudinal motion simulation result is as in figure 9.

3.2. Morphing

Lateral morphing occurs as the angle between the arms of the quadcopter UAV decreases. The changes that occur with the effect of contraction are given in Table 4. While the intersection angle is 45°, the width of the aircraft is 86 mm and the length is 207 mm. This causes the I_x and I_y values to change. Pitch degree of 2° is given for the longitudinal movement of the aircraft after contraction. The simulation results are as follows (Figure 10).

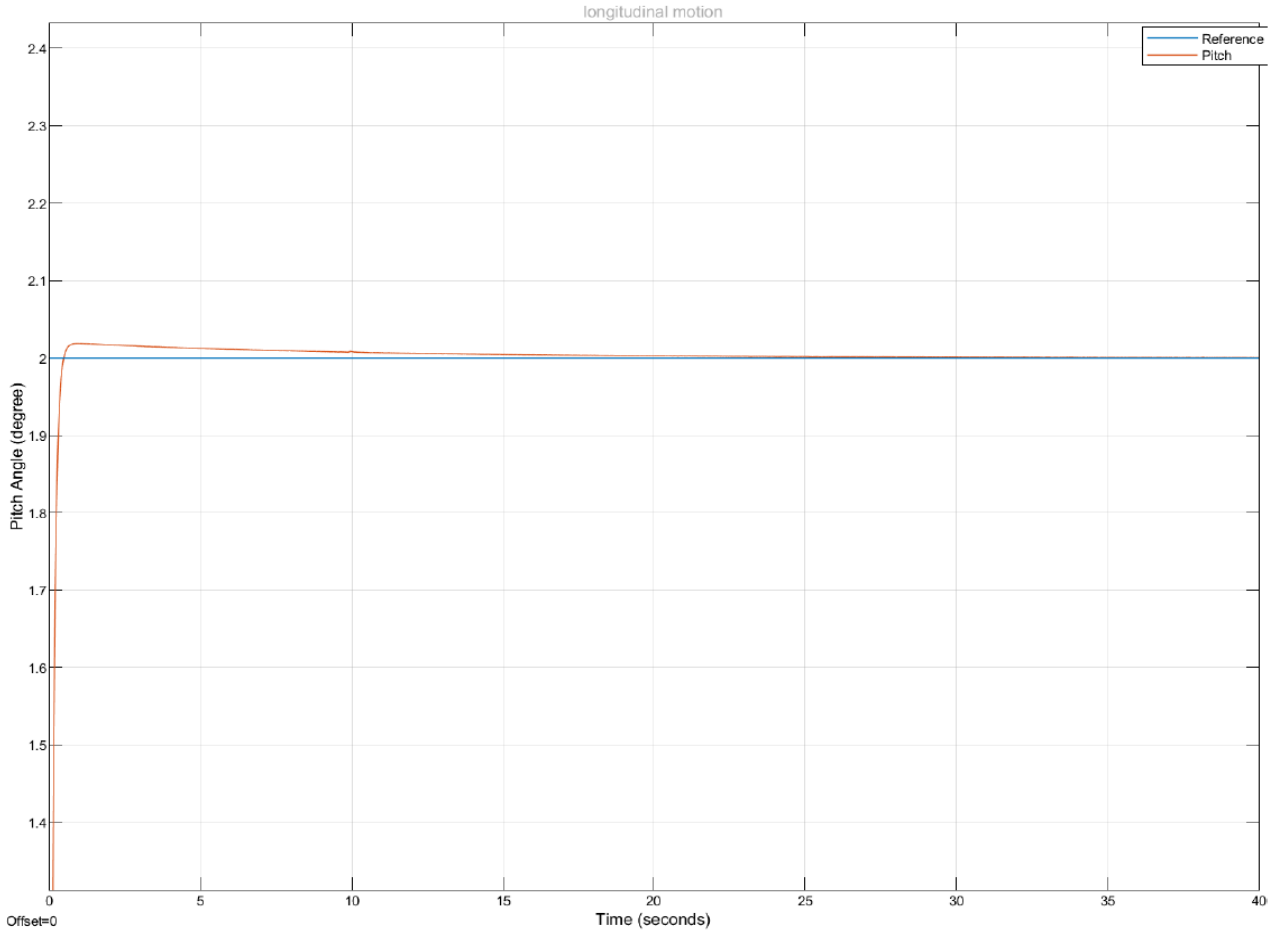

Figure 10. Forward Movement (Intersection Angle; 45°)

The effect of shape changes on performance, rise time, settling time and overshoot values in the simulation carried out are shared in the table.

Table 4. General Dimensions and Performance Criteria of the Aircraft

Symbol	Non-Morphing	Morphing	Unit
∠ /2	90	45	degree
I_x	0.005	0.003	kgm^2
I_y	0.005	0.008	kgm^2
I_z	0.009	0.009	kgm^2
Rise Time	1.403	1.765	s
Settling Time	13.9	10.3	s
Overshoot	14.773 %	6.989 %	

Since this work is related to lateral flight. different deformation is created by decreasing or increasing the intersection angle between the arms at different times. As the volume of the quadcopter changes during the conversion process. there are also changes in the moments of inertia.

Lateral movement is the movement of the quadcopter on the x-axis. U_2 given in equation (8) is applied as input for the quadcopter to perform its lateral movement. In the state space model. Ø is shown as the output for the lateral movement. The Simulink model. designed for a 2° pitch angle longitudinal. was examined under the headings of non-morphing and morphing .

3.3. Non Morphing

Simulated in MATLAB / SIMULINK using the values given in the Table without changing the intersection angle between the arms of the aircraft. Matlab The block diagram in SIMULINK is as shown in the figure. Input data were obtained from u.w.q . pitch . X.Y graphs by entering the state space model.

In the simulation. an angle of 2° is given as a reference value. Longitudinal movement PID values P=50; I=5; Values were entered as D=50 by making use of previous studies (Oktay et al.. 2017). The graph was obtained by running the simulation for 40 seconds. Lateral motion simulation result is as in figure 11.

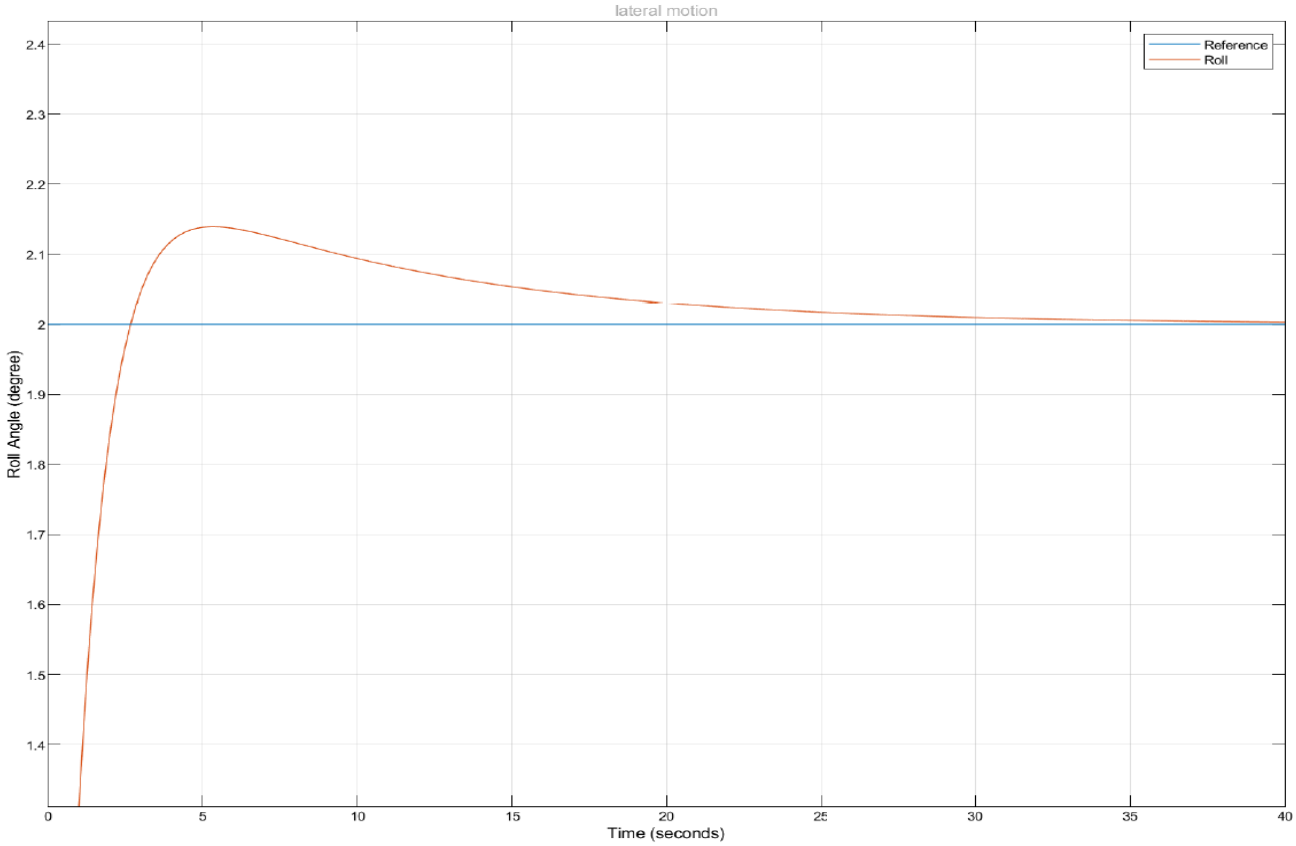

Figure 11. Lateral Movement (Intersection Angle 90°). PID (50.5.50)

3.4. Morphing

Lateral morphing occurs as the angle between the arms of the quadcopter UAV decreases. The changes that occur with the effect of contraction are given in Table 5. While the intersection angle is 45°. the width of the aircraft is 86 mm and the length is 207 mm. This causes the I_x and I_y values to change. An angle of 2° is given for the lateral movement of the aircraft after contraction. The simulation results are as follows.

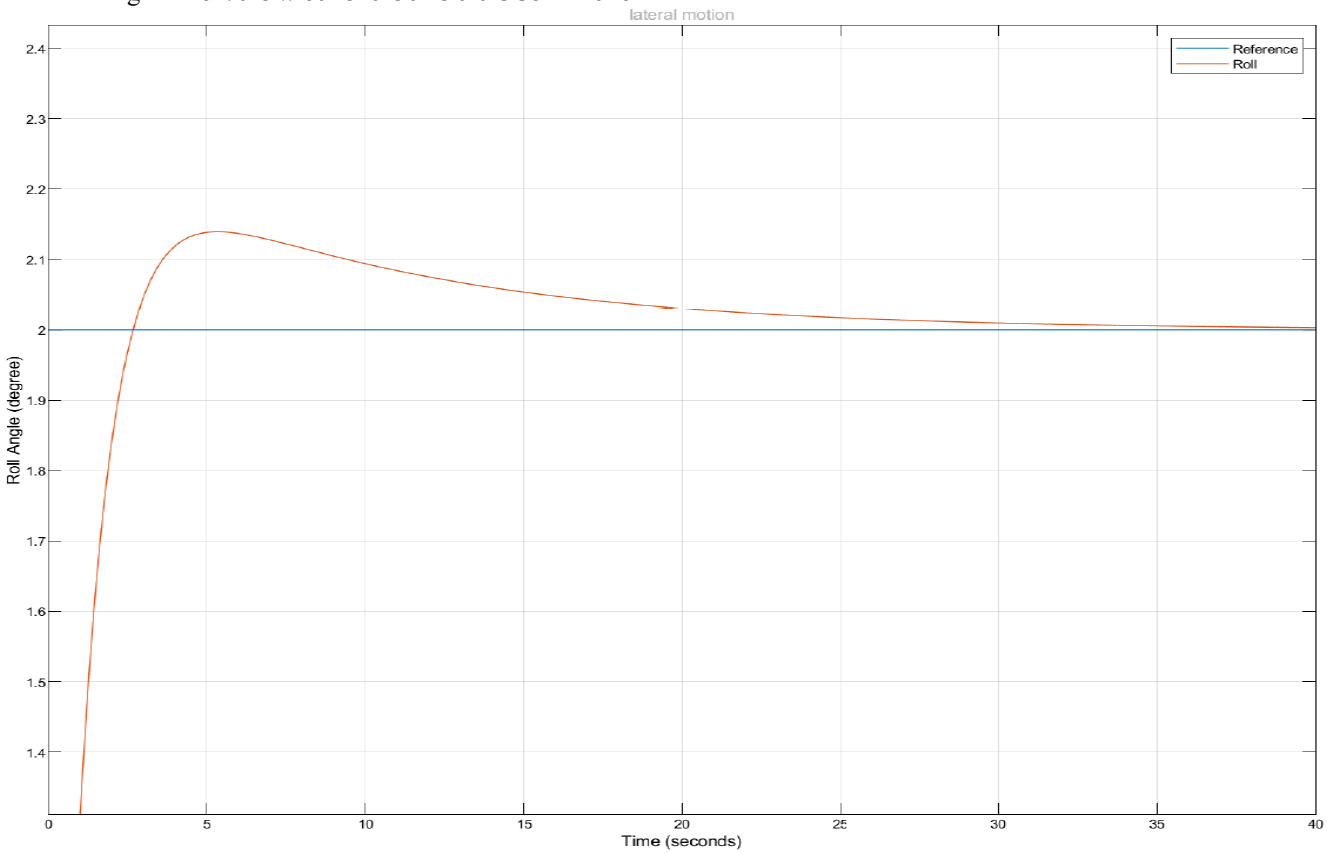

Figure 12. Lateral Movement (45° Intersection Angle)

The effect of shape changes on performance. rise time. settling time and overshoot values in the simulation carried out are shared in the table.

Table 5. General Dimensions and Performance Criteria of the Aircraft

Symbol	Non-Morphing	Morphing	Unit
∠ /2	90	45	degree
I_x	0.005	0.003	kgm^2
I_y	0.005	0.008	kgm^2
I_z	0.009	0.009	kgm^2
Rise Time	1.437	1.402	s
Settling Time			
Overshoot	13.830 %	14.773 %	

4. Conclusion

In this study. the actively morphing aircraft X1 (non-morphing) and X2 (morphing) can fly in two different configurations. The geometry. mass and moments of inertia were obtained from the study designed in the CATIA program for the X1 and X2 configurations. In the next section. the state space model for the aircraft's lateral flight is constructed. It was simulated in MATLAB/SIMULINK environment and the results of rise. overshoot and settling times were compared.

The change in the intersection angle of the aircraft changes the moment of inertia values as given in Table 2. This change is also shown graphically (Figure 5-6) in the simulation studies. It has been seen that greater moment force is needed to perform the pitching motion. that is. the forward motion. increasing I_y as a result of the pitching of the intersection angle of the aircraft from 90° to 45°. It has been determined that the aircraft settles to the reference value and performs its movement when the study is carried out in a noise-free environment.

Changing the intersection angle of the aircraft changes the moment of inertia values as given in Table 3. This change is also shown graphically (Figure 2-3) in the simulation studies. It has been observed that smaller moment force is needed to realize the reduced I_x lateral movement as a result of the rolling of the intersection angle of the aircraft from 90° to 45°. It has been determined that the aircraft settles to the reference value and performs its movement when the study is carried out in a noise-free environment.

In this study. the dynamics of a rotary wing quadcopter aircraft were investigated. A PID controller has been verified in simulation studies to be well adapted to the aircraft while hovering. PID coefficients used for forward motion in the study of O. Köse and T. Oktay ; 12.12.5 are given. Scope data obtained in this study (Figure 6). equivalent data were obtained. Data from different PID values were shared (Figure 6). The PID controller was able to control the aircraft when it was hovering and in the absence of atmospheric noises. It was observed that the overshoot value and the rise time increased when the umbilical angle was 45°. In future studies. the effects of lateral movement and different configurations will be examined.

In this study. the dynamics of a rotary wing quadcopter aircraft were investigated. A PID controller has been verified in simulation studies to be well adapted to the aircraft while hovering. PID coefficients used for forward motion in the study of O. Köse and T. Oktay; 1.1.1.1.1.65 are given (Oktay et al.. 2020). The PID controller was able to control the aircraft when it was hovering and in the absence of atmospheric noises. It was observed that the overshoot value increased and the rise time decreased when the umbilical angle was 45°. In future studies. the behavior of longitudinal and lateral movements in noisy environments will be examined using different PID coefficients. and maximum control and stability behaviors.

Ethical approval

Not applicable.

Conflicts of Interest

The authors declare that there is no conflict of interest regarding the publication of this paper.

References

Bai. Y. Gururajan. S. (2019). Evaluation of A Baseline Controller For Autonomous “Figure-8” Flights Of A Morphing Geometry Quadcopter: Flight Performance. Drones 2019. 3. 70

Coban. S. Bilgic. H. H. & Akan. E. (2020). Improving Autonomous Performance of a Passive Morphing Fixed Wing UAV. Information Technology and Control. 49(1). 28-35.

Çoban S. Bilgiç H.H. Oktay T. (2019). Designing. dynamic modeling and simulation of ISTECOPTER. Journal of Aviation. 3 (1). 38-44. DOI: 10.30518/jav.564376

Desbiez. A. Expert. F. Boyron. M. Diperi. J. Viollet.S. Ruffier. F. (2017). X-Morf: A Crash-Separable Dört Pervaneli That Morfs Its X-Geometry in Flight. 2017 Workshop on Research. Education And Development Of Unmanned Aerial systems (red uas)

Di Luca M. Mintchev S. Heitz G. Noca F. Floreano D. (2017). Bioinspired Morphing Wings for Extended Flight Envelope And Roll Control Of Small Drones. Interface Focus 7: 20160092.

Eraslan. Y. Özen. E. Oktay. T. (2020) A Literature Review on Determination of Dört Pervaneli Unmanned Aerial Vehicles Propeller Thrust and Power Coefficients. Ejons X – International Conference on Mathematics – Engineering – Natural & Medical Sciences Proceeding Book. 2020 Batumi. Georgia

Eraslan. Y. Özen. E. Oktay. T. (2020) The Effect of Change in Angle Between Rotor Arms on Trajectory Tracking Quality of A Pid Controlled Quadcopter. Ejons X – International Conference on Mathematics – Engineering – Natural & Medical Sciences Proceeding Book. 2020 Batumi. Georgia

Falanga. D. Kleber. K. Mintchev. S. Floreano. D. Scaramuzza. D. (2018) The Foldable Drone: A Morphing Dört Pervaneli That Can Squeeze and Fly. IEEE Robotics and Automation Letters. Preprint Version. Accepted November. 2018

J. Boulet. (1991). Histoire De l’Hélicoptère. France-Empire.

Kekeç E.T. Konar M. Dalkıran F. (2020). Sportif Havacılık İçin Düşük Maliyetli. Kullanışlı Variometre Tasarımı Ve Gerçekleştirimi J. Aviat. 4 (1). 79-88.

Köse O. Oktay T. (2020 Investigation of The Effect of Differential Morphing on Forward Flight by Using PID Algorithm in Quadcopters J. Aviat. 4 (1). 15-21.

Köse.O. Oktay.T.(2021) İnovatif Yöntemlerle Kuadkopter Modellenmesi. Kontrolü Ve Gerçek Zamanlı

Uygulamaları. Doktora Tezi. Erciyes Üniversitesi. Fen Bilimleri Enstitüsü. KAYSERİ

Oktay. T. & Sal. F. (2016). Combined Passive and Active Helicopter Main Rotor Morphing for Helicopter Energy Save. Journal Of The Brazilian Society Of Mechanical Sciences And Engineering. 38(6). 1511-1525

Oktay. T. Özen. E. (2021). Döner Kanatlı İnsansız Hava Aracının Sistem Tasarımı Ve Kontrolü. Avrupa Bilim Ve Teknoloji Dergisi. (27). 318-324.

Oktay.T. Özen. E. (2021). Kapalı Ortamlarda Arama Kurtarma Görevi İçin Gelistirilen Şekil Değistirebilen Quadcopterin Sistem Modellemesi Ve Tasarımı. Mas 14th International European Conference on Mathematics. Engineering. Natural&Medical Sciences March 26-28. 2021/Széchenyi István University/HUNGARY

Prisacariu. V. Sandru. V. & Rău. C. (2011). Introduction Morphing Technology in Unmanned Aircraft Vehicles (UAV). Paper Presented at The International Conference of Scientific Paper. AFASES.

Oktay. T. Uzun. M. Çelik. H. Konar. M. (2017). Pid Based Hierarchical Autonomous System Performance Maximization of a Hybrid Unmanned Aerial Vehicle (Huav). Anadolu University Journal of Science and Technology A- Applied Sciences and Engineering

Cite this article: Özen. E. Oktay. T. (2022). Effects of Shape Changing of Morphing Rotary Wing Aircraft on Longitudinal and Lateral Flight. Journal of Aviation. 6(3). 251-259.